17th Brazilian Congress of Thermal Sciences and Engineering
November 25th-28th, 2018, Águas de Lindóia, SP, Brazil

ENCIT-2018-0422
NUMERICAL SIMULATION OF THE TWO-DIMENSIONAL INCOMPRESSIBLE FLOW AROUND ELLIPTIC CYLINDERS USING THE VORTEX METHOD

Vanessa G. Guedes
Special Technology Department, Electrical Energy Research Center (CEPEL). Av. Horácio Macedo, 354 - Rio de Janeiro - Brazil.
vanessa.g@cepel.br

Rodrigo R. S. Pereira
Mechanical Engineering Department, Federal University of Rio de Janeiro. Av Athos da Silveira Ramos, 149 - Centro de Teconologia, Ilha do Fundão, RJ, Brazil.
rodrsp@poli.ufrj.br

Carolina W. Araújo
Mechanical Engineering Department, Federal University of Rio de Janeiro. Av Athos da Silveira Ramos, 149 - Centro de Teconologia, Ilha do Fundão, RJ, Brazil.
Athos da Silveira Ramos, 149.

Gustavo C. R. Bodstein
Mechanical Engineering Department, Federal University of Rio de Janeiro. Av Athos da Silveira Ramos, 149 - Centro de Teconologia, Ilha do Fundão, RJ, Brazil.
Athos da Silveira Ramos, 149.

Abstract. E*xternal incompressible flows around bluff bodies are characterized by different regimes that depend mainly on the body geometry and the value of the Reynolds number, ranging from steady Stokes-type flows to strongly unsteady turbulent flows. For large Reynolds numbers a Von Karman-type periodic wake is formed as a result of boundary layer separation and vortex shedding. In this the mesh-free two-dimensional vortex method utilized to simulate two-dimensional, incompressible, unsteady flows taken into account for obtaining the numerical results is discussed. Flow around bluff bodies, in specific around circular cylinders, are also important for testing numerical algorithms. A comparison with experimental and other numerical studies of flow from the literature is made to validate the algorithm.*
Lamb vortices are generated near the cylinder surface, whose strengths are determined to ensure that the no-slip condition is satisfied and that circulation is conserved. The impermeability condition is imposed through the application of a source panel method, so that mass conservation is explicitly enforced. The vorticity dynamics of the body wake is computed using the convection-diffusion splitting algorithm, where diffusion is simulated using the random walk method and convection is carried out with a lagrangian second-order time-marching scheme. Results for the time history of the aerodynamic coefficients on the body surface are presented and compared to other results available in the literature, showing good agreement.

Keywords: *Incompressible Flow, Elliptic Cylinder, Vortex Method, Panel Method, High Reynolds Number*

1. INTRODUCTION

Flows around bluff bodies are characterized by the occurrence of massive boundary layer separation and the formation of a turbulent periodic wake downstream of the body. These complex phenomena make the numerical prediction of these flows very difficult, and one has to rely on specific experimental data to calculate the aerodynamic forces on the body. The study of external incompressible flows at high Reynolds numbers around bluff bodies finds extensive applications to real-life engineering problems.

In this paper, the formulation of the vortex method associated with a source panel method (Mustto, *et al*, 1998 and Mustto and Bodstein, 2011) to simulate two-dimensional, incompressible, unsteady flows is discussed. Flows around bluff bodies, in specific around circular cylinders – which are traditional in the literature –, are also important for testing numerical algorithms. A comparison with experimental and other numerical studies of flows is made to validate the algorithm.

An important application of elliptic cylinders is in heat exchangers. This recent surge of interest is partly due to their smaller flow resistance compared to a circular cylinder (Khan, *et al*, 2005 and Faruquee, *et al*, 2007). This implies in

considerably smaller pumping requirements when using elliptic tubes instead of circular ones. Moreover, the smaller frontal area of elliptic tubes results in more compact heat exchanger design and is also beneficial in terms of particulate fouling of the outer surface in applications where severe fouling conditions prevails. The smaller frontal area and the reduced vortex shedding of the elliptic-shaped tube causes less particle deposition due to inertial impaction (Khan, *et al*, 2004 and Bouris, *et al*, 2001). After performing experiments with three bundle arrangements, Bouris, *et al* (2001) showed that the in-line bundle with elliptic-shaped tubes presents the lowest fouling rates and pressure drop.

The objective of this work is to use the vortex method associated with a source panel method (Guedes, *et al*, 2004 and Roy and Bandyopadhyay, 2006) to simulate two-dimensional, incompressible, unsteady flows past elliptic cylinders aligned and inclined to the incident flow.

2. COMPUTATIONAL PROCEDURE

The flowfield is calculated as the sum of a uniform flow, a cloud of Lamb vortices that model the vorticity in the boundary layer and wake, and a series of straight panels containing piecewise-continuous linear-strength source distributions that discretize the body surface. In our mesh-free vortex method, Lamb vortices are generated along the cylinder surface, whose strengths are determined to ensure that the non-slip condition is satisfied and that circulation is conserved. The impermeability condition is imposed through the application of the source panel method (Anderson, 1981, Guedes et al., 2004), so that mass conservation is explicitly enforced. Vortices generated near the body surface evolve with time in a lagrangian manner to make up the body wake. Vorticity dynamics in the rotational region is computed using the convection-diffusion splitting algorithm, where convection and diffusion are calculated sequentially in time. The convective transport of vorticity is calculated with the Adams-Bashforth second-order time-marching scheme, whereas the diffusive transport of vorticity is simulated using the random walk method. Kamemoto (2004) presents an algorithm that also uses source panels to calculate the normal velocity on the body surface, but the treatment of the vorticity generation process is different from the present algorithm. In Kamemoto's algorithm, a thin vorticity layer with a specified height is created along the body surface and diffuses into the flowfield as a rectangular boundary element. As this element reaches a certain distance normal to the boundary, it turns into a circular vortex blob. In order to keep higher accuracy, a vorticity redistribution schemes is implemented.

A flow around an elliptic cylinder of length 2*a*, height 2*b* and aspect ratio $\xi \equiv a/b$, immersed in an unbounded region with a uniform flow of freestream speed *U* is considered (Fig. 1).

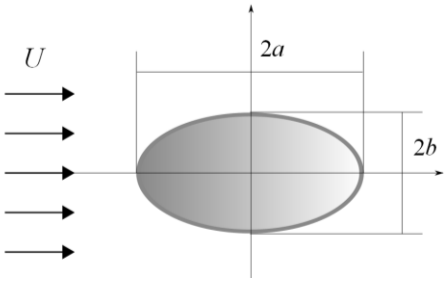

Figure 1. Flow around an elliptic cylinder

The flow is assumed as incompressible and two-dimensional, and the fluid as newtonian with constant kinematic viscosity ν. The unsteady flow that develops originates from the boundary layer separation on the cylinder surface, which generates an oscillatory wake downstream of the body. This flow is governed by the continuity and the Navier-Stokes equations nondimensionalized by *U* and 2*a*, written as:

$$\nabla \cdot \mathbf{u} = 0 \quad \text{and} \quad \frac{\partial \mathbf{u}}{\partial t} + \mathbf{u} \cdot \nabla \mathbf{u} = -\nabla p + \frac{1}{Re} \nabla^2 \mathbf{u} \tag{1, 2}$$

In which $Re \equiv 2Ua/\nu$ is the Reynolds number based on the height of the elliptic cylinder.

For all cases studied, the flow is started impulsively from rest. The impermeability and the no-slip boundary conditions on the surface of the cylinder and the condition at infinity can be expressed in terms of the velocity field as:

$$u_n \equiv \mathbf{u} \cdot \mathbf{n} = 0 \ \text{ and } \ u_t \equiv \mathbf{u} \cdot \mathbf{t} = 0 \text{, on the cylinder surface.} \tag{3, 4}$$

$$|\mathbf{u}| \to 1 \text{, at infinity.} \tag{5}$$

In our model, the flow vorticity is represented by a cloud of *Nv* Lamb vortices, each of strength Γj and core radius σ. The contribution to the flow due to the presence of the body is accounted for using a piecewise-continuous linear-source panel method (Anderson, 1991), where the body surface is divided into *Np* straight panels, each of strength λj. We superimpose the flows comprised of the vortex cloud, the uniform flow and the flow due to the source panels to construct a flow field that satisfies Eq. (1), Eq. (3) and Eq. (5) automatically. Thus, the *u* and *v* velocity components of the total flow in the *x* and *y* directions, respectively, can be written in terms of the unknown vortex and source strengths, and the known panel geometry, according to the following equations:

$$u(x,y) = cos\alpha + \sum_{j=1}^{Np} \frac{\lambda_j}{2\pi}\left(\frac{C_u}{2} ln\left(\frac{Sp_j^2+2A Sp_j+B}{B}\right) + \frac{D_u - AC_u}{E}\left(tan^{-1}\frac{Sp_j+A}{E} - tan^{-1}\frac{A}{E}\right)\right) - \sum_{k=1}^{Nv}\frac{\Gamma_k}{2\pi}\frac{(y-y_k)}{(x-x_k)^2+(y-y_k)^2}\left\{1 - exp\left[-C\frac{(x-x_k)^2+(y-y_k)^2}{\sigma^2}\right]\right\} \tag{7a}$$

$$v(x,y) = sin\alpha + \sum_{j=1}^{Np} \frac{\lambda_j}{2\pi}\left(\frac{C_v}{2} ln\left(\frac{Sp_j^2+2A Sp_j+B}{B}\right) + \frac{D_v - AC_v}{E}\left(tan^{-1}\frac{Sp_j+A}{E} - tan^{-1}\frac{A}{E}\right)\right) + \sum_{k=1}^{Nv}\frac{\Gamma_k}{2\pi}\frac{(x-x_k)}{(x-x_k)^2+(y-y_k)^2}\left\{1 - exp\left[-C\frac{(x-x_k)^2+(y-y_k)^2}{\sigma^2}\right]\right\} \tag{7b}$$

In which α is the angle of attack, C = 5.02572 is a constant and the remaining constants in Eq. (7a) and Eq. (7b) can be written in terms of the geometrical coordinates and orientation of the panels, presented in Fig. 2, as:

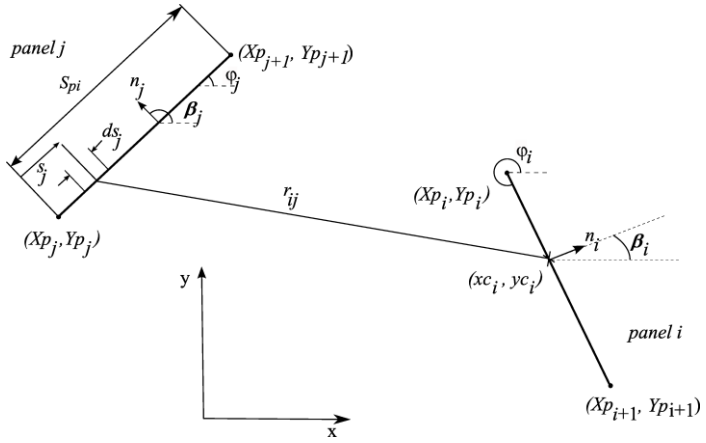

Figure 2. Geometry of the panels

$$A = -(x - Xp_j)cos\,\varphi_j - (y - Yp_j)sin\,\varphi_j \text{ and } B = (x - Xp_j)^2 + (y - Yp_j)^2 \tag{8a, b}$$

$$C_u = -cos(\varphi_j) \text{ and } D_u = x - Xp_j \tag{8c, d}$$

$$Sp_j = \left((Xp_{j+1} - Xp_j)^2 + (Yp_{j+1} - Yp_j)^2\right)^{1/2} \text{ and } E = \left(B - A^2\right)^{1/2} = (x - Xp_j)sin\varphi_j - (y - Yp_j)cos\,\varphi_j \tag{8e, f}$$

$$C_v = -sin(\varphi_j) \text{ and } D_v = y - Yp_j \tag{8g, h}$$

Equations (7) and (8) are used to calculate the induced velocities at any point in the flow, including the panel control points and the vortices in the wake cloud.

The aerodynamic force coefficients are calculated through the integration of the pressure coefficient distribution on the surface of the elliptic cylinder, and may be expressed as:

$$C_D = \int_0^{2\pi\left(\frac{1}{2}(a^2+b^2)\right)^{\frac{1}{2}}} C_p \sin(\varphi - \alpha)\,(s)\,ds \tag{9}$$

$$C_L = \int_0^{2\pi\left(\frac{1}{2}(a^2+b^2)\right)^{\frac{1}{2}}} C_p \cos(\varphi - \alpha)\,(s)\,ds \tag{10}$$

The pressure coefficient, *Cp*, on a panel control point (*xci*, *yci*) is calculated according to the following expression:

$$C_p = 1 + 2\left(\sum_{k=1}^{m}\frac{\Gamma_k}{\Delta t} - \sum_{k=1}^{n_{max}}\frac{\Gamma_k}{\Delta t}\right) \tag{11}$$

The two-dimensional, incompressible, unsteady flow around an elliptic cylinder formulated above is solved using a vortex method based on the algorithm devised by Chorin (1973) that splits the convective-diffusive operator in the form:

$$\frac{D\omega}{Dt} \equiv \frac{\partial\omega}{\partial t} + \mathbf{u}\cdot\nabla\omega = 0 \quad \text{and} \quad \frac{\partial\omega}{\partial t} = \frac{1}{Re}\nabla^2\omega \tag{12a,b}$$

In which *n* and *t* are unit vectors in a direction normal and tangential to the cylinder surface, respectively.

The vortex method utilized simulates the transport of vorticity by convection and diffusion in a sequence within the same time step, such that the simulated solution converges to the solution of the vorticity equation when Δt tends to zero.

First, the convective process, governed by Eq. (12a), is calculated through the lagrangian motion of each vortex. This step is accomplished by integration in time of each vortex path equation employing to the second-order Adams-Bashforth scheme (Guedes, 2003), given by the following equations:

$$\Delta x_c = \left[\frac{3}{2}u(t) - \frac{1}{2}u(t-\Delta t)\right]\Delta t \quad \text{and} \quad \Delta y_c = \left[\frac{3}{2}v(t) - \frac{1}{2}v(t-\Delta t)\right]\Delta t \tag{13a,b}$$

The Adams-Bashforth scheme is used because it is faster than the Runge-Kutta scheme, for the same Δt.

The process of viscous diffusion, governed by Eq. (12b), is simulated using the Random Walk Method (Lewis, 1991). The random displacements of each vortex in the *x* and *y* directions owing to diffusion, Δx_d and Δy_d, are calculated from

$$\Delta x_d = \Delta r\cos(\Delta\theta) \quad \text{and} \quad \Delta y_d = \Delta r\sin(\Delta\theta) \tag{14a,b}$$

$$\Delta r = \left[4Re^{-1}\Delta t\ln(1/P)\right]^{1/2} \quad \text{and} \quad \Delta\theta = 2\pi Q \tag{15a,b}$$

We estimate the vortex core radius σ by its growth during a time step Δt, that is, $\sigma = 4.48\,(\Delta t/Re)1/2$. The distance ε from the cylinder surface where the nascent vortices are generated per time step is set equal to σ (Fig. 3). Vortices that penetrate the body are reflected back into the flow. Considering a convective velocity scale of order one and a length scale of the order of the average panel length, the time step Δt can be estimated from $\Delta t = (2k/Np)(1+\xi)$, where $0 < k \leq 2$ is a numerical parameter that limits the convective step of each vortex.

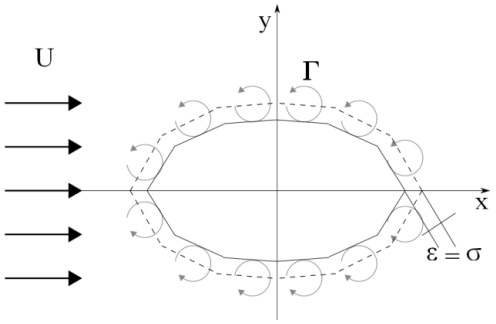

Figure 3. Vortex generation scheme

Measurements are made for different aspect ratios and incident angles. Results for a high Reynolds number incompressible flow around two-dimensional elliptic cylinders of aspect ratios of 0.25, 0.50 and 2.00, aligned to the incoming flow are presented; and results obtained for an elliptic cylinder of aspect ratio of 0.50, with attack angles of 5°, 10°, 15° and 30°.

3. ALGORITHM VALIDATION

To validate the algorithm, the case of a circular cylinder immersed in a uniform, two-dimensional, incompressible, unsteady flow, with a high Reynolds number is chosen. This flow is simulated using $Np = 128$, $\Delta t = 0.05$, and $\varepsilon = \sigma = 0.0032$. Figure 4 shows the wake pattern behind the cylinder that illustrates the vortex shedding mechanism and the velocity field near the circular cylinder.

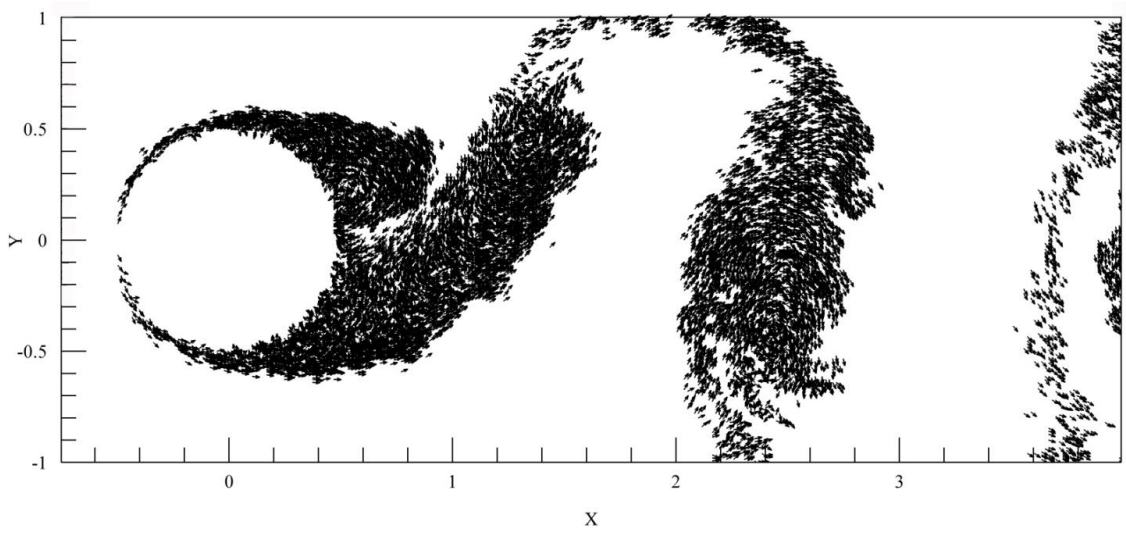

Figure 4. Velocity field in the circular cylinder downstream wake for $Re = 1 \times 10^5$.

The values of the Strouhal number, *St*, and the mean drag and lift coefficients are presented in Table 1 compared to the experimental results.

Table 1. Algorithm validation results for flow around circular cylinder for $Re = 10^5$.

Results	C_D	C_L	*St*
Present simulation: vortex method with source panels and without turbulence	1.400	0.002	0.204
Mustto and Bodstein (2011): vortex method with vortex panels and turbulence model	1.483	-	0.199
Guedes (2003): vortex method with source panels and without turbulence	1.270	-0.570	0.195
Pereira, *et al* (2003): vortex method with vortex panels and turbulence model	1.210	0.040	0.240
Pereira, *et al* (2003): vortex method with vortex panels without turbulence model	1.120	0.050	0.270
Mustto, *et al* (1998): vortex method with images and without turbulence model	1.220	-	0.220
Blevins (1984): experimental	1.200	-	0.190

As the simulations show, the numerical results obtained provide the correct physical description of the flow and the calculated quantities are overall in agreement with the experimental results used for comparison. There are, however, some discrepancies that have been observed in some cases. We point out that the numerical calculation of massively separated flow is expected to be difficult due to the flow complexity.

4. RESULTS AND DISCUSSION

In addition to the Reynolds number, flow around an elliptic cylinder is strongly dependent on its aspect ratio and angle of attack. In what follows, results are presented for $\alpha = 0^o$, three values of the aspect ratio and Reynolds number: $\xi = 0.25$ and $Re = 4\times105$ (Case I), $\xi = 0.5$ and $Re = 2\times10^5$(Case II); $\xi = 0.8$ and $Re = 5\times10^4$ (Case III).All simulations

were run up to t=50 with the following numerical parameters: Np= 128, Δt= 0.05for cases I, II and III and ε=σ= 0.0016 (Case I); ε=σ= 0.0022 (Case II); ε=σ= 0.0045 (Case III).

Figure 5 illustrates the velocity field at the final step (t = 50) of all simulated cases. The time histories of the lift and drag coefficients are plotted in the graphs of Fig. 6.

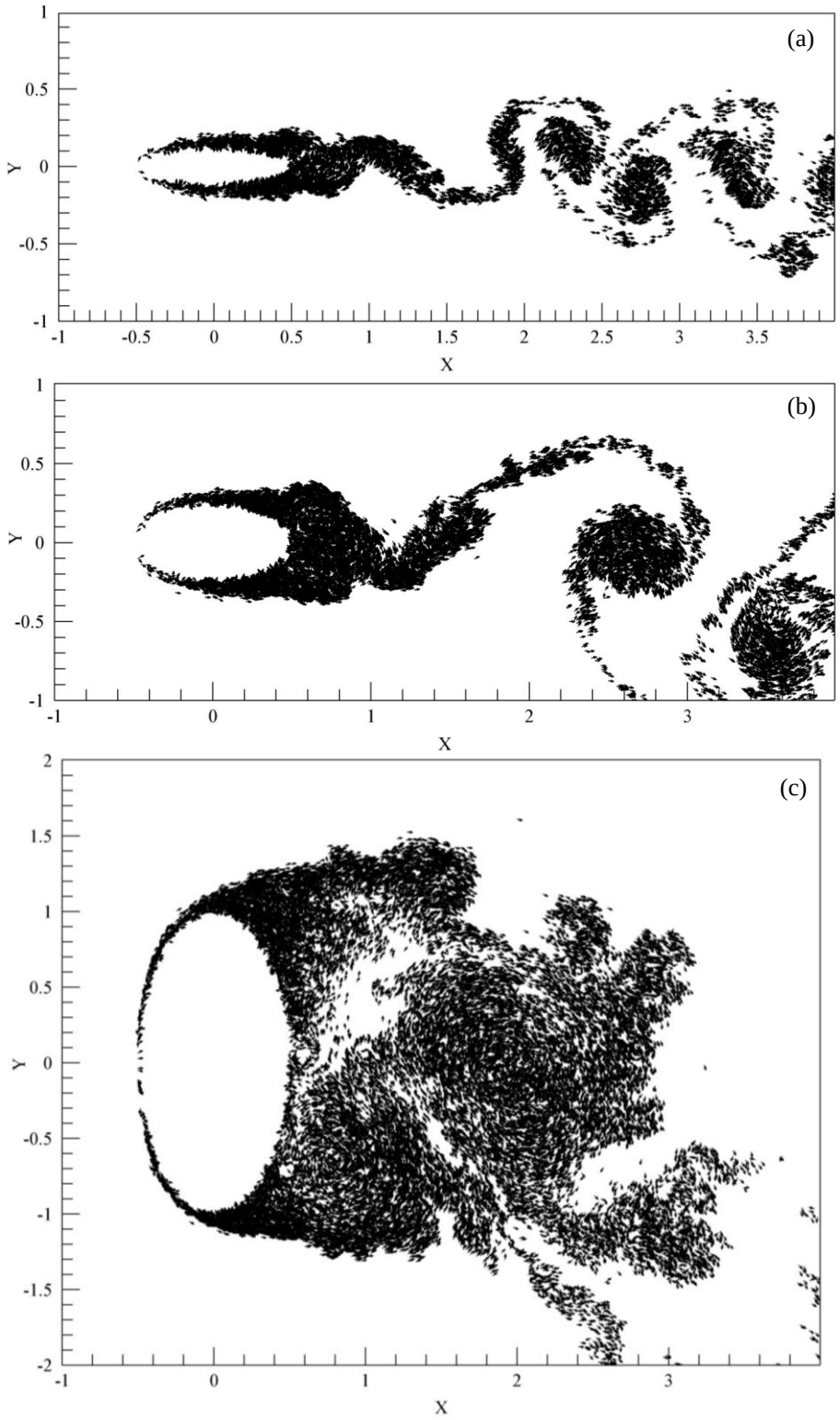

Figure 5. Velocity field around an elliptic cylinder as a function of the aspect ratio.
(a) Case I: ξ = 0.25, α = 0º, Re = 4×10^5; (b) Case II: ξ = 0.5, α = 0º, Re = 2×10^5;
(c) Case III: ξ = 2.0, α = 0º, Re = 5×10^4.

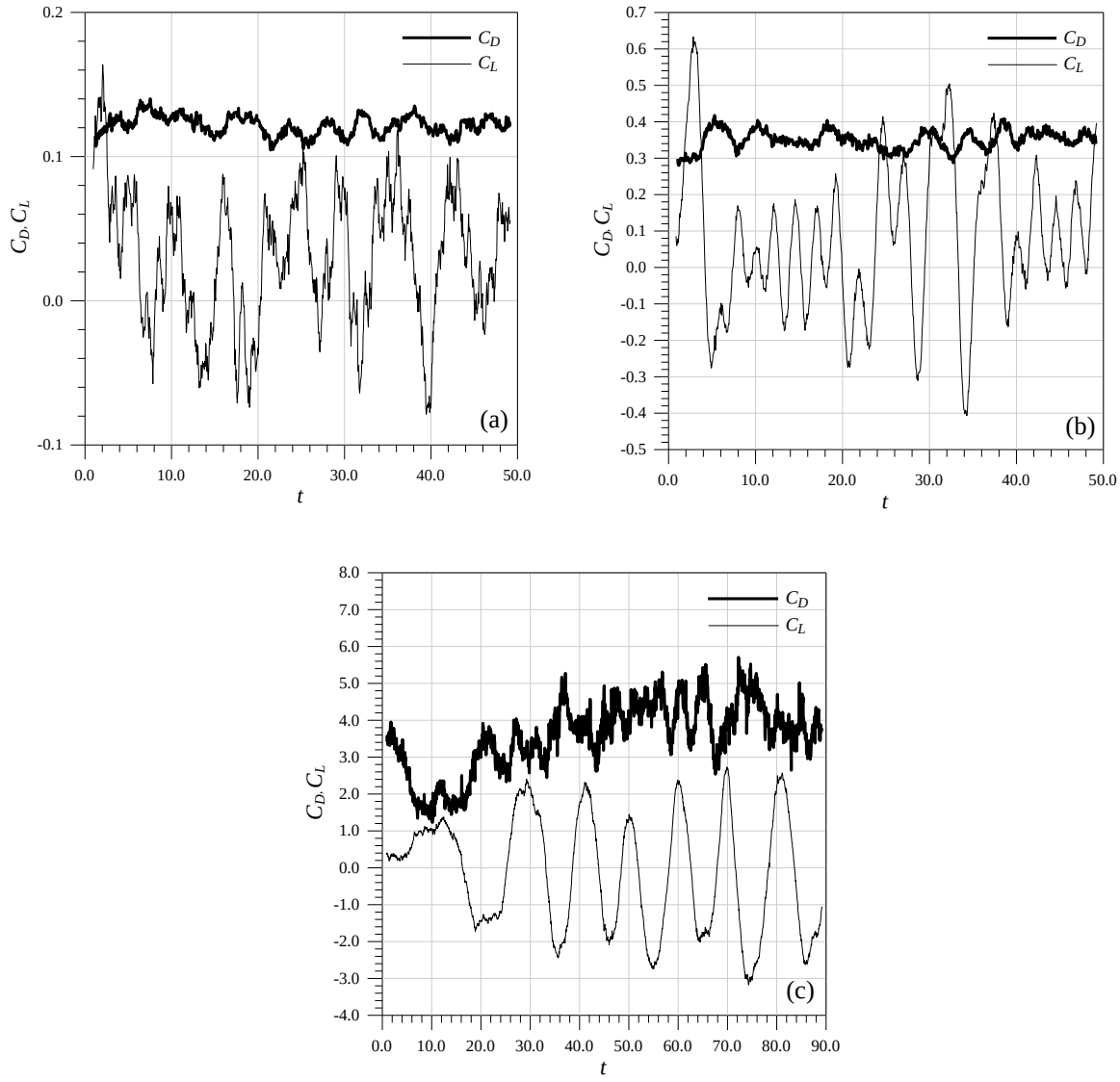

Figure 6. Time history of C_D and C_L.
(a) Case I: $\xi = 0.25$, $\alpha = 0^o$, $Re = 4\times10^5$; (b) Case II: $\xi = 0.5$, $\alpha = 0^o$, $Re = 2\times10^5$;
(c) Case III: $\xi = 2.0$, $\alpha = 0^o$, $Re = 5\times10^4$.

Table 2 provides a way to compare our numerical results for the drag coefficient and Strouhal number to other experimental and numerical results available in the literature.

Table 2. Comparison of the mean drag coefficient and Strouhal number with other numerical and experimental results.

Results	***Aspect Ratio***	***Re***	***C_D***	***St***
Blevins (1984): experimental	0.25	4×10^5	0.08	0.20 – 0.30
Carreiro and Bodstein (2002): numerical	0.25	1×10^4	0.21	0.93
Present results: numerical	0.25	4×10^5	0.12	0.18
Blevins (1984): experimental	0.50	2×10^5	0.30	0.20 – 0.30
Carreiro and Bodstein (2002): numerical	0.50	1×10^4	0.49	0.46
Present results: numerical	0.50	2×10^5	0.35	0.40
Blevins (1984): experimental	2.00	5×10^4	3.20	0.20 – 0.30
Present results: numerical	2.00	5×10^4	4.05	0.10

We now consider several cases of an elliptic cylinder set at a non-zero angle of attack α with respect to a uniform freestream flow with $Re = 1\times10^5$. Simulations for $\alpha = 5^o$, 10^o, 15^o and 30^o and $\xi = 0.5$ were made. The results of Choi and Lee (2001) for C_L and St, measured with $h/b = 1.5$, $\xi = 0.5$ and $Re = 1.36 \times 10^4$, are shown in Fig. 7, superimposed to the present results for $\xi = 0.5$ and $Re = 1\times10^5$, without ground effect ($h/b = \infty$).

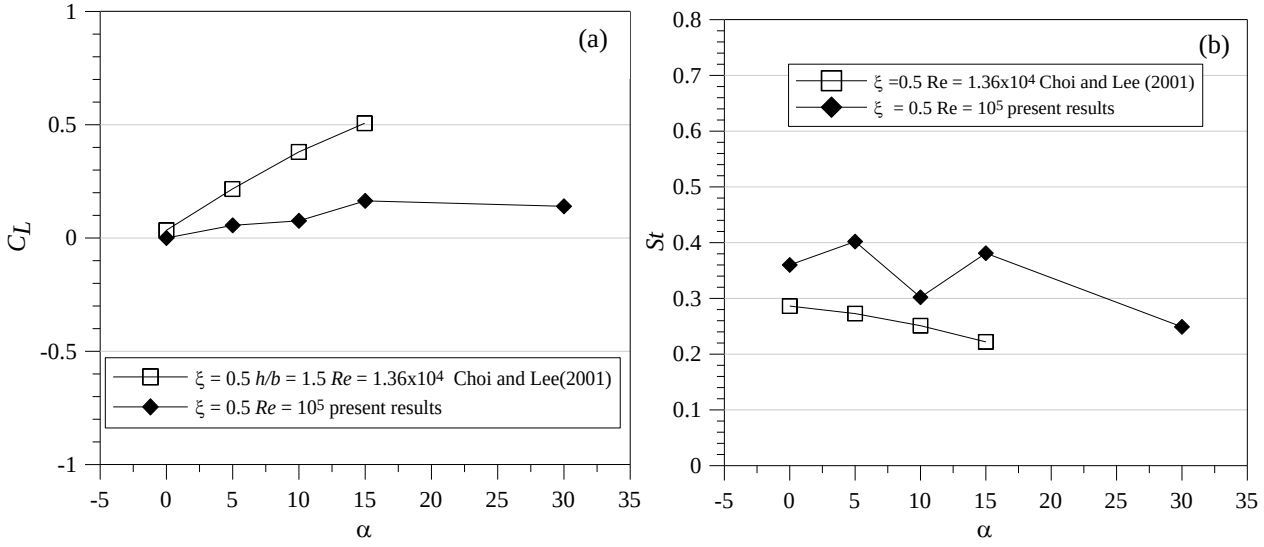

Figure 7. C_L and St variation in function of α for ξ= 0.5.
(a) $C_L \times \alpha$; (b) $St \times \alpha$.

Figure 8 shows velocity-vector plots to illustrate the variation in time of the velocity field around an elliptic cylinder of aspect ratio of 0.5 at an incidence angle of 30º. These figures are shown for five different times each of which corresponds to a quarter of a cycle to one whole cycle of oscillation in the period from $t = 13$ to $t = 17$. These five times are marked up on the graph for the time variation of the aerodynamic coefficients, also shown in Fig. 5.

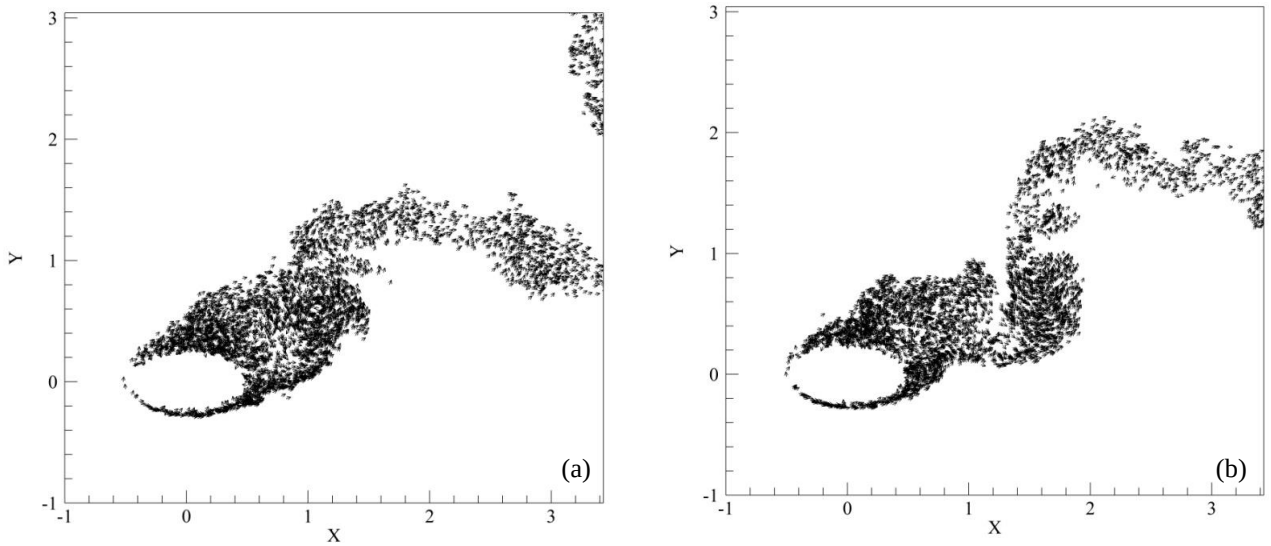

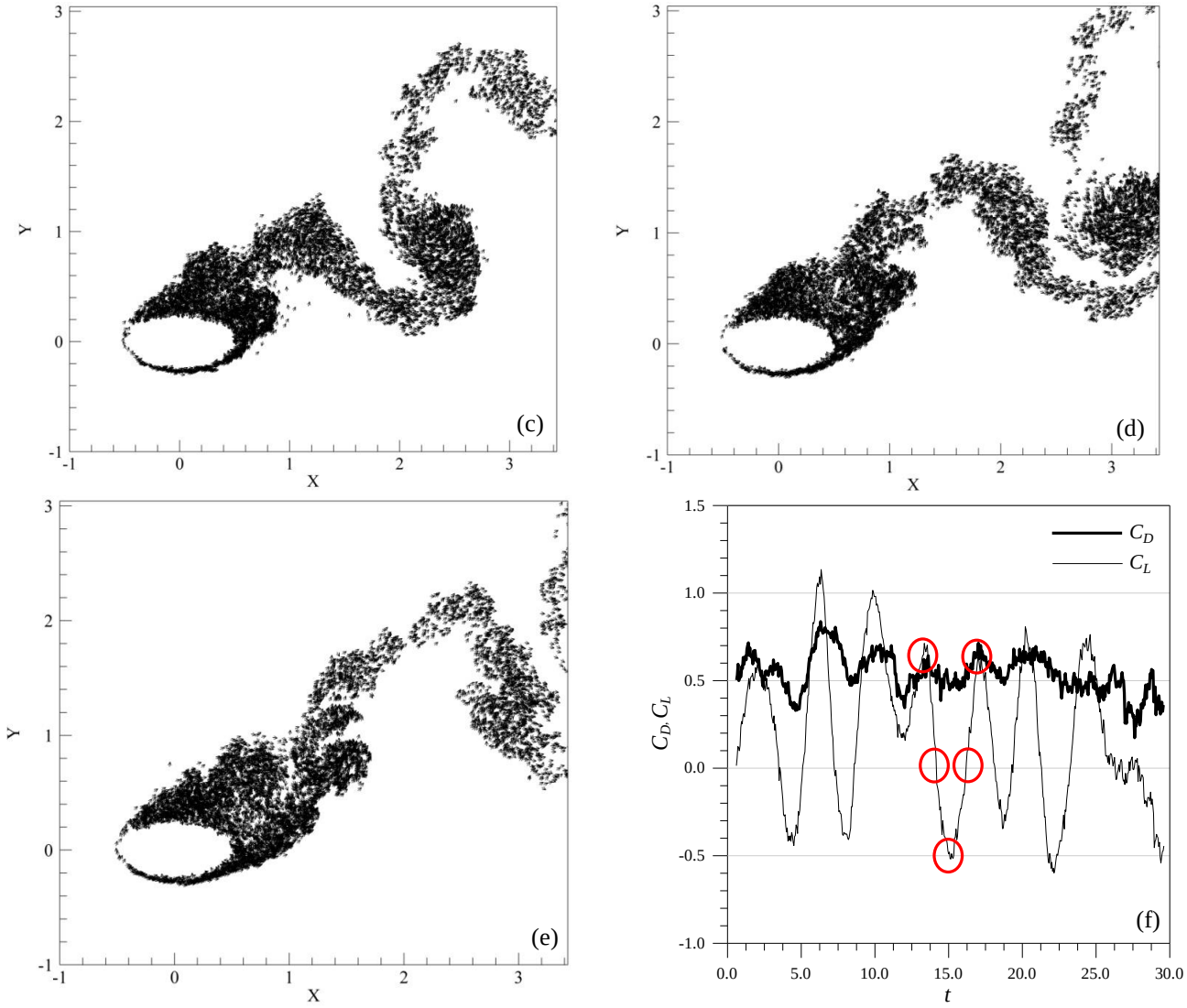

Figure 8. Velocity field around an elliptic cylinder of aspect ratio of 0.5 at an incident angle of 30º for instants of time from t = 13 to t = 17. (a) t = 13 (260 steps); (b) t = 14 (280 steps); (c) t = 15 (300 steps); (d) t = 16 (320 steps); (e) t = 17 (340 steps); (f) Time history of C_D and C_L.

5. CONCLUSIONS

As the simulations show, the numerical results obtained provide the correct physical description of the flow and the calculated quantities are overall in agreement with the experimental results used for comparison. There are, however, some discrepancies that have been observed in some cases. We point out that the numerical calculation of massively separated flow is expected to be difficult due to flow complexity. Although the algorithm has proven to be effective to simulate massively separated flows around elliptic cylinders, the numerical results suggest that an increase in the resolution of the simulation, through an increase in the number of vortices, may improve the accuracy of the simulation. Three-dimensional effects, present in the experiments, may only be accounted for through the use of a three-dimensional model.

6. REFERENCES

Anderson J.D., 1991. *Fundamentals of Aerodynamics.* McGraw Hill, 2nd Edition.
Blevins, R.D., 1984. *Applied Fluid Dynamics Handbook.* Van Nostrand Reinhold Co, 1st Edition.

Bouris, D., Papadakis, G. and Bergeles, G., 2001. "Numerical evaluation of alternate tube configurations for particle deposition rate reduction in heat exchanger tube bundles." *International Journal of Heat Fluid Flow.* Vol. 22, p. 525–536.

Carreiro, F.R. and Bodstein, G.C.R., 2002. "Simulação Numérica do Escoamento Não-Permanente em Torno de Cilindros Elípticos Via Transformação de Joukowsky." In *Proceedings of 9th Brazilian Congress of Thermal Engineering and Sciences. 15-18 October 2002*. Minas Gerais, Brazil, p. 1-10.

Choi, J.H. and Lee, S.J., 2001. "Flow characteristics around na inclined elliptic cylinder in a turbulent boundary layer." *Journal of Fluids and Structures.* Vol. 15, p. 1123-1135.

Chorin A.J., 1973. "Numerical Study of Slightly Viscous Flow." *Journal of Fluid Mechanics*. Vol 57, p. 785-796.

Faruquee, Z., Ting, D.S.K., Fartaj, A., Barron, R.M. and Carriveau, R., 2007. "The effects of axis ratio on laminar fluid flow around an elliptical cylinder." *International Journal of Heat and Fluid Flow*.Vol. 28, p. 1178–1189.

Guedes V.G. 2003. *Numerical Simulations of flow around circular and rectangular cylinders using the vortex method.* D.Sc. thesis, COPPE/UFRJ, Rio de Janeiro.

Guedes VG, Bodstein GCR and Hirata MH (2004). "Numerical Simulation of the flow around a square cylinder using the vortex method." *Revista de Engenharia Térmica 3:* No. 2, p. 161-167.

Kamemoto K. (2004). "On contribution of Advanced Vortex Element Methods toward virtual reality of unsteady vortical flows in the new generation o CFD." *Journal of the Brazillian Society of Mechanical Sciences & Engineering XXVI*: No.4, p. 368-378.

Khan, M.G., Fartaj, A. and Ting, D.S.K., 2004. "An experimental characterization of cross-flow cooling of air via an in-line elliptical tube array." *International Journal of Heat Fluid Flow*. Vol. 25, p. 636–648.

Khan, W.A., Culham, J.R. and Yovanovich, M.M., 2005. "Fluid flow around and heat transfer from elliptical cylinders: analytical approach." *Journal of Thermophysics and Heat Transfer.* Vol. 19, p. 178–185.

Lewis R.I., 1991. *Vortex Element Methods for Fluid Dynamic Analysis of Engineering Systems.* Cambridge University.

Mustto A.A., and Bodstein G.C.R., 2011. "Subgrid-Scale Modeling of Turbulent Flow Around Circular Cilinder by Mesh-Free Vortex Method." *Engineering Applications of Computational Fluid Mechanics* Vol. 5, p. 259-275.

Mustto A.A., Hirata M.H. and Bodstein G.C.R., 1998. "Discrete Vortex Method Simulation of the flow around a circular cylinder with and without rotation." In *Proceedings of the 16th AIAA Applied Aerodynamics Conference. June 15-18, 1998,* Albuquerque, NM, USA, 1, p. 59-69.

Pereira L.A.A., Hirata, M.H.H. and Silveira Neto A., 2003. "Vortex Method with Sub-grid Scale Modelling." *Journal of the Brazillian Society of Mechanical Sciences & Engineering XXV* Vol. 2, p. 1-12.

Roy A and Bandyopadhyay G (2006). "Numerical calculation of separated flow past a circular cylinder using panel technique." *Journal of Wind Engineering and Industrial Aerodynamics 94*, p. 131-149.

7. RESPONSIBILITY NOTICE

Vanessa G. Guedes, Rodrigo R. S. Pereira, Carolina W. Araújo, Gustavo C. R. Bodstein are the only responsible for the printed material included in this paper.